THE EPED PEDESTAL MODEL: EXTENSIONS, APPLICATION TO ELM-SUPPRESSED REGIMES, AND ITER PREDICTIONS

by
P.B. SNYDER, T.H. OSBORNE, M.N.A. BEURSKENS,
K.H. BURRELL, R.J. GROEBNER, J.W. HUGHES,
R. MAINGI, R. NAZIKIAN, D. ORLOV, O. SCHMITZ,
M.R. WADE, J.R. WALK and H.R. WILSON

GENERAL ATOMICS

DISCLAIMER

THE EPED PEDESTAL MODEL: EXTENSIONS, APPLICATION TO ELM-SUPPRESSED REGIMES, AND ITER PREDICTIONS

by
P.B. SNYDER, T.H. OSBORNE, M.N.A. BEURSKENS,[1]
K.H. BURRELL, R.J. GROEBNER, J.W. HUGHES,[2]
R. MAINGI,[3] R. NAZIKIAN,[4] D. ORLOV,[5] O. SCHMITZ,[6]
M.R. WADE, J.R. WALK[2] and H.R. WILSON[7]

[1]EURATOM /CCFE Fusion Association, Culham Science Centre, Abingdon, UK
[2]Massachusetts Institute of Technology, PSFC, Cambridge, Massachusetts USA
[3]Oak Ridge National Laboratory, Oak Ridge, Tennessee USA
[4]Princeton Plasma Physics Laboratory, Princeton, New Jersey USA
[5]University of California San Diego, La Jolla, California USA
[6]Forschungszentrum Jülich, Germany
[7]York Plasma Institute, Dept of Physics, University of York, UK

GENERAL ATOMICS PROJECT 03726
SEPTEMBER 2012

GENERAL ATOMICS

ABSTRACT

The pressure at the top of the edge transport barrier (or "pedestal height") strongly impacts global confinement and fusion performance, while large ELMs can significantly limit component lifetimes. Hence, accurately predicting the pedestal height in ITER, as well as developing a predictive understanding of ELM suppression, are essential. The EPED model predicts the H-mode pedestal height and width based upon two fundamental and calculable constraints: (1) onset of non-local peeling-ballooning (P-B) modes at low to intermediate mode number, and (2) onset of nearly local kinetic ballooning modes (KBM) at high mode number. The model calculates both constraints directly with no fit parameters, using ELITE to calculate the P-B constraint, and a "BCP" technique, informed by gyrokinetic calculations, to calculate the KBM constraint. EPED has been successfully compared to observed pedestal height for 270 cases on 5 tokamaks, finding agreement within ~20%. Recent results include successful testing of EPED in Quiescent H-Mode discharges, and the development of a working model to understand ELM suppression by resonant magnetic perturbations (RMPs). Dynamically, the ELM crash is typically followed by a recovery, in which the pressure gradient encounters the KBM limit, but the pedestal can continue to broaden until the P-B boundary is reached, an ELM is triggered, and the cycle repeats. The ELM can be suppressed if this recovery phase is interrupted such that the width of the edge barrier is prevented from continuing to broaden. We propose an EPED-based working model for suppression of ELMs by RMPs in which the conceptual "wall" is provided by a resonant island or stochastic region that drives strong transport and prevents inward pedestal propagation. This leads to predictions of specific profile changes and ranges of q in which ELM suppression is possible, which agree with initial tests on DIII-D. EPED predictions for ITER have been made for more than 100 baseline and hybrid cases, finding a high pedestal that is further optimized at high density. The "Super H-Mode" regime, predicted to be accessible via dynamic optimization, is also discussed, including the possibility of access to this regime in ITER.

High performance ("H-mode") in tokamaks is achieved via the spontaneous formation of an insulating transport barrier in the outer few percent of the confined plasma. The pressure at the top of the edge transport barrier (or "pedestal height") strongly impacts global confinement and fusion performance, with fusion power in ITER predicted to scale approximately with the square of the pedestal height [1]. However, the substantial free energy in the edge pedestal can drive large edge localized modes (ELMs) which can significantly limit component lifetimes in ITER-scale devices [2]. The EPED model [3–5] predicts the H-mode pedestal height and width based upon two fundamental and calculable constraints: (1) onset of non-local peeling-ballooning (P-B) modes at low to intermediate mode number, (2) onset of nearly local kinetic ballooning modes (KBM) at high mode number. The model calculates both constraints directly with no fit parameters, using ELITE to calculate the P-B constraint, and a "BCP" technique to calculate the KBM constraint [3]. EPED has been successfully compared to observed pedestal height for 270 cases on 5 tokamaks, finding agreement within ~20% [3–8]. Here we briefly discuss the EPED model, recent experimental tests, application to ELM-suppressed regimes, ITER predictions, and ongoing model development.

The present version of the EPED model proceeds from the conjecture that, while many mechanisms drive transport across the edge transport barrier region (ETB) in high performance H-mode discharges, the mechanisms which are strong enough to ultimately limit the pressure gradient, and total pressure, in the presence of strong sources and very strong ExB shear typical of the ETB, are the KBM and P-B. The P-B and KBM constraints are calculated using ELITE [9,10] and the BCP technique [3] on series of model equilibria, as shown in Fig. 1(a), yielding predictions of pedestal height and width (black circle). As part of a 2011 US research milestone, EPED was extensively tested in a set of dedicated experiments on Alcator C-Mod and DIII-D, in which the magnetic field, current, density and shape were varied, yielding large variation in pedestal height and width. On DIII-D, a new higher resolution Thomson system allowed very high accuracy measurements of both height and width. Figure 1(b) shows an example of a detailed test of the model using this new system. In this series of 3 discharges, the plasma current (I_p) was varied by a factor of 3 (0.5, 1.0, 1.5 MA), with the magnetic field (B_T) and plasma shape fixed. The calculated peeling-ballooning constraint [solid line, Fig. 1(b)] increases roughly linearly with current, with its increase slowing at lower q (higher current). The calculated KBM constraint (dotted line) increases more strongly with current, roughly as I_p^2. As a result of the interaction of the KBM and P-B constraints, the EPED predicted pedestal height rises strongly (~3x) with I_p as it is increased from 0.5 to 1.0 MA. However, the predicted height saturates and the width decreases dramatically as I_p is increased from 1.0 to 1.5 MA. The model predictions for both height and width are in reasonable agreement with the observations (red squares) for all three values of the current, successfully predicting the complex observed changes in height and width (changes which would not be described by a simple scaling law, or by P-B physics alone). In a broader statistical comparison, EPED predictions of the pedestal width were compared to a set of 24 cases from 14 shots with widths measured by the new DIII-D Thomson system. As shown in Fig. 1(c) (blue circles), agreement between the predicted and observed width is good, with a ratio of 0.94±0.13, and a correlation coefficient r=0.91 between predicted and observed width [and similar agreement in predicted height, as shown by blue circles in
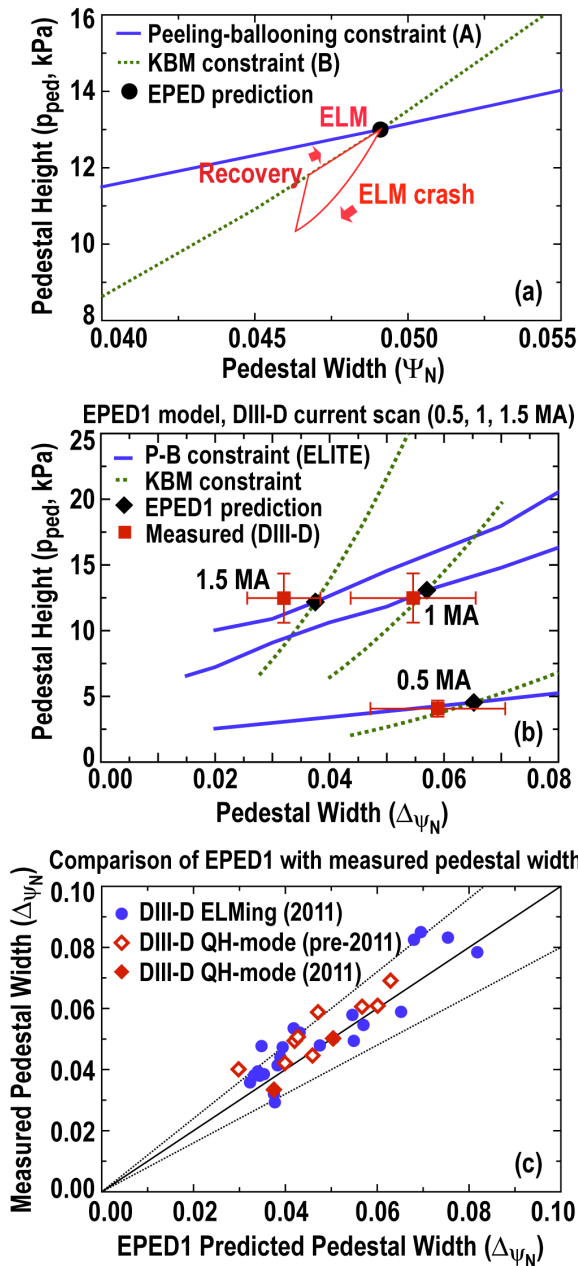
FIG. 1. (a) EPED predicts the pedestal height and width (black circle) as the intersection of calculated peeling-ballooning (solid line) and KBM (dotted line) constraints. A typical ELM cycle in this space is illustrated in red. (b) EPED predicted height and width (black diamonds) is compared to observations (red squares) for a current scan across 3 discharges on DIII-D. (c) Comparison of EPED predicted and observed pedestal width for a set of DIII-D discharges with accurate width measurements from a new Thomson system (blue circles) as well as from a set of 11 QH-mode discharges (diamonds).

Fig. 2(a)]. An extensive set of experiments was conducted in ELMing H-mode discharges on Alcator C-Mod, varying the magnetic field (3.4, 5.3, 8 T) and the plasma current and density, and measuring pedestal structure with high resolution Thomson scattering [8]. Comparisons of measured pedestal structure to EPED find similar agreement as on DIII-D, as shown in Fig. 2(a) (green crosses). These comparisons extend tests of the model up to pressures within ~3x of predicted ITER pressure [black diamond Fig. 2(a)], and to B_T and density equal to and exceeding ITER values. A similarity experiment was conducted on DIII-D, matching the C-Mod shape and dimensionless parameters, and found similar agreement with the model [blue + symbols in Fig. 2(a)].
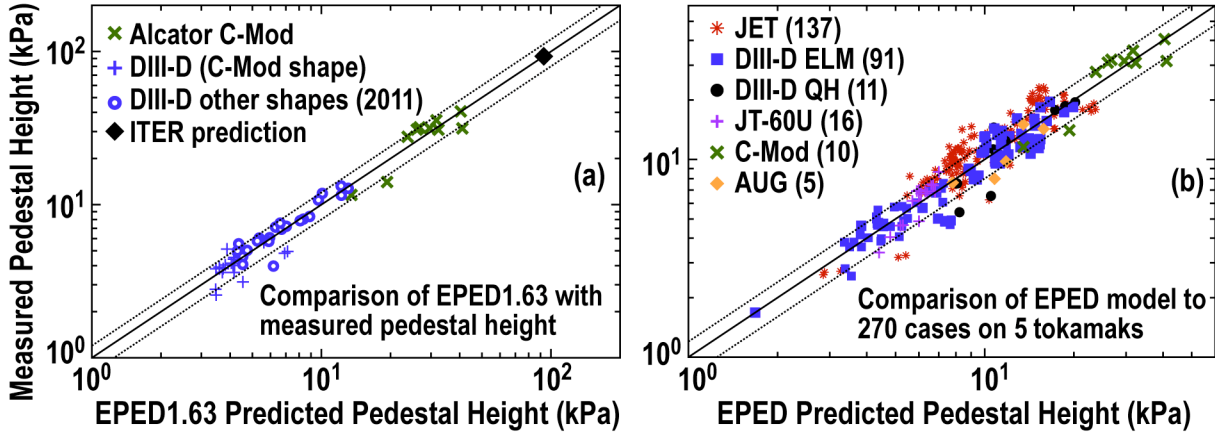
FIG. 2. (a) Comparison of EPED predicted pedestal height to observations on Alcator C-Mod and DIII-D, including a similarity experiment on C-Mod and DIII-D. An EPED prediction for the ITER baseline is also shown. (b) Comparison of predicted and observed pedestal height for a set of 270 cases on five tokamaks.

Combining these recent tests of the EPED model with results from an extensive comparison to JET [7], as well as additional comparisons to AUG, DIII-D, and JT-60U [3–7], yields a dataset of 270 cases on 5 tokamaks, shown in Fig. 2(b). For this set of cases, the ratio of predicted to observed pedestal height is 0.98 ± 0.20, with a correlation coefficient $r=0.92$. Statistically, this is consistent with ~10%–15% measurement error and EPED accuracy to within ~15%–20%. Observed trends in pedestal height with I_p, B_T, plasma shape and density are generally well captured by the model.

The EPED model has been extensively used to predict the pedestal height and width in various scenarios on ITER, with more than 100 cases considered (e.g. [3,5]). Because ITER performance is expected to depend strongly on pedestal height, optimization in various scenarios is expected to be very important. An example study of predicted ITER pedestal pressure vs. density at 2 different I_p values is shown in Fig. 3(a). Notably, the pedestal height is predicted to increase with pedestal density up to quite high values, exceeding the Greenwald density limit. Understanding this limit, as well as ensuring sufficient fuelling capability to reach high density may be important for ITER optimization. Work on parametrizing the EPED results for ITER [11] and on combining these predictions with calculations of core transport and stability and boundary physics is ongoing. Initial indications are that a combined pedestal-core optimization of ITER should enable it to attain fusion performance in the range of its established goals.

One interesting aspect of the EPED model is that it predicts the existence of a regime in which very high pedestal pressure is possible, known as "Super H-Mode". An example, for strongly shaped DIII-D-like parameters, is shown in Fig. 3(b). For any value of the pedestal density, the standard EPED prediction (white lines) has a single value. However, for strongly shaped discharges, a second, or "Super H-Mode" region is potentially accessible via a dynamic optimization of the density (starting at moderate density and then raising the density to high values after the pedestal is fully developed). The EPED model predicts this regime should be accessible in high triangularity DIII-D, JET and ITER discharges, and there are preliminary indications of possible partial access on DIII-D and JET. For example, it has been observed in

high triangularity JET discharges that when strong gas puffing is used to increase the pedestal density, high pedestal pressures, somewhat in excess of the standard EPED predictions, can be achieved [7,12], which may indicate at least partial access to the Super H-Mode regime. An example calculation for ITER baseline parameters is shown in Fig. 3(c). A small amount of access to Super H-Mode is predicted to be possible at high density in ITER, and this access can likely be enhanced via optimization of shape and safety factor. Further study of possible Super H-Mode access is planned.
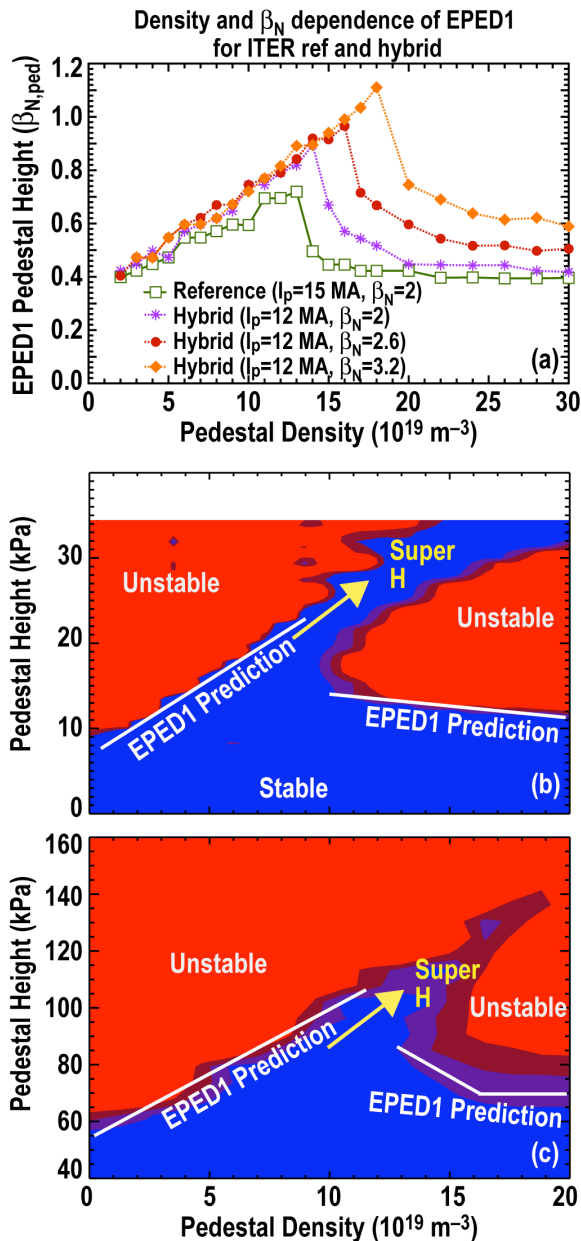

FIG. 3. (a) EPED predictions for ITER pedestal height as a function of pedestal density for ITER baseline (15 MA) and hybrid (12 MA) cases. (b) EPED predictions for pedestal height (white lines) are shown as a function of pedestal density for a high triangularity DIII-D case. Note in particular that a "Super H-Mode" region at very high pedestal pressure is potentially accessible by starting at lower density and then dynamically increasing the density in time to move up and to the right in this parameter space. (c) A similar diagram as (b), but for ITER baseline parameters, exhibiting a small but significant region of access to Super H-mode conditions at high density in ITER.

In addition to understanding the physics of pedestal structure in ELMing discharges, it is important to understand the physics of ELM-suppressed regimes, such as Quiescent H-mode (QH) [13], and ELM suppression by resonant magnetic perturbations (RMP) [14]. The EPED

model has recently been applied to QH-mode discharges, finding similar agreement in predicted pedestal width and height as in ELMing discharges [red diamonds in Fig. 1(c), and black asterisks in Fig. 2(b)] [4]. This is consistent with earlier studies finding that the edge harmonic oscillation (EHO) in QH-mode is driven near the kink-peeling part of the P-B stability boundary [10], and with local gradients constrained by KBM.

To understand RMP ELM-suppression it appears necessary to consider the dynamic ELM cycle, illustrated for example by the red lines and arrows in Figs. 1(a) and 4(a). The ELM (or EHO in QH-mode) is predicted to occur near the black circle, and the ELM can be prevented if the recovery part of the cycle is stopped, such that the pedestal does not continue to broaden and/or grow. We hypothesize that in RMP ELM suppression, broadening of the pedestal can be prevented by penetration of the RMP near the pedestal top. This requires a precise location of the RMP penetration, and offers an explanation for observed q-windows for ELM suppression and narrowing of the pedestal during ELM suppression [4]. As an example, a series of DIII-D RMP experiments with varying safety factor q_{95} are shown in Fig. 4(b). For the parameters in these discharges, the EPED model predicts a critical pedestal width of ~3–3.5% (the predicted critical width varies slightly in different cases because the EPED input parameters, including shape, current and pedestal density vary). That is, with the pressure gradient constrained by the KBM, the peeling-ballooning mode is expected to go unstable when the width exceeds this critical value. When the RMPs are not applied [filled circles in Fig. 4(b) show the width shortly before an ELM], the width rises to or above the critical value and ELMs are triggered. When the RMP is turned on and ELMs are suppressed [open diamonds in Fig. 4(b)], the width remains below the critical value. When the RMP is on and small ELMs occur, the width, within measurement uncertainty, reaches the critical value. Note also that in Fig. 4(b), and other DIII-D observations, ELM suppression occurs in "windows" of q_{95} values. Investigation of several
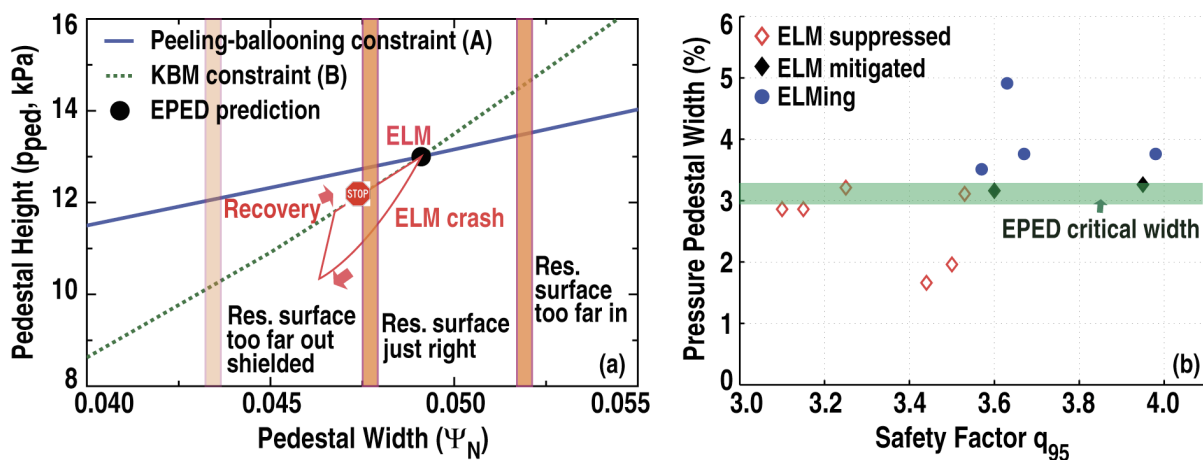

FIG. 4. (a) A working model for RMP ELM suppression is illustrated, showing that a region of increased transport (here associated with a rational surface, e.g. an island or stochastic region) can suppress the ELM if this region is in the proper location to constrain the broadening of the pedestal. (b) Measured pressure pedestal width is shown as a function of safety factor for a series of DIII-D discharges. Filled circles show discharges with no RMP (and ELMs). Open diamonds show cases with the RMP on and full ELM suppression, while filled diamonds show cases with the RMP on and small ELMs present.

cases indicates that these windows correspond to values of q_{95} in which a rational surface (typically 9/3, 10/3, 11/3 or 12/3) lies near the top of the pedestal, in a region where enhanced magnetic transport could potentially limit the broadening of the pedestal and suppress the ELM, as in Fig. 4(a). Substantial work is ongoing to study the physics of RMP penetration, and identify conditions for penetration of magnetic structures into the plasma [15–17]. Much additional work is needed to fully quantify this RMP working model, but initial observations do suggest the presence of magnetic structures near the top of the pedestal in ELM-suppressed cases [17], consistent with this working model.

The success of the EPED model has generated further interest in direct electromagnetic gyrokinetic (EMGK) studies of the pedestal region. EPED uses a simplified ballooning critical pedestal (BCP) technique to calculate the KBM constraint [3], which has been compared in several cases with direct EMGK calculations with codes such as GYRO [18], GS2 [19] and GEM [20]. In the "first stable" regime for the KBM, these comparisons are relatively straightforward, and the BCP technique reproduces EMGK calculations with reasonable accuracy. However, with strong shaping, low collisionality and/or high-q, plasmas can achieve a significant degree of second stability access to the KBM. While the BCP technique in EPED attempts to account for this, purely local EMGK calculations likely cannot be used to determine the KBM threshold in this limit. It is expected, based on MHD theory and simulation, that finite-n (non-local) effects are important. Initial work is ongoing with both local and non-local EMGK calculation to quantify the KBM in both first and 2nd stable regimes, as well as to study other relevant microinstabilities in the pedestal region.

In summary, the EPED model has been developed and extensively tested on several tokamaks, finding ~20% agreement with observed pedestal height and width. The model has been successfully tested on ELMing and QH-mode discharges, and used in the development of a working model for RMP ELM suppression. Further model development and testing are ongoing, including electromagnetic gyrokinetic calculations and consideration of direct incorporation of such calculations in the model. ITER pedestal predictions with the EPED model have been made for a wide range of conditions, and these predictions are being integrated with predictions of core transport and other important physics to assess and optimize overall fusion performance of the ITER device.

REFERENCES

[1]   KINSEY, J.E., *et al.*, Nucl. Fusion **31** (2011) 083001.

[2]   LOARTE, A., *et al.*, Plasma Phys. Control. Fusion **45** (2003) 1549.

[3]   SNYDER, P.B., *et al.*, Nucl. Fusion **51** (2011) 103016.

[4]   SNYDER, P.B., *et al.*, Phys. Plasmas **19** (2012) 056115.

[5]   SNYDER, P.B., *et al.*, Phys. Plasmas **16** (2009) 056118; Nucl. Fusion **49** (2009) 085035.

[6]   GROEBNER, R.J., *et al.*, Nucl. Fusion **50** (2010) 064002; Nucl Fusion **49** (2009) 085037.

[7]   BEURSKENS, M., *et al.*, Phys. Plasmas **18** (2011) 056120; H-Mode workshop (2011).

[8]   WALK, J.R., *et al.*, Nucl. Fusion **52** (2012) 063011.

[9]   WILSON, H.R., *et al.*, Phys. Plasmas **9** (2002) 1277.

[10] SNYDER, P.B., *et al.*, Phys. Plasmas **9** (2002) 2037; Nucl. Fusion **47** (2007) 961.

[11] POLEVOI, A.R., *et al.*, "Simplified Pedestal Parameterization Based on EPED1 Simulations for ITER-like Plasmas," ITER report ITER_D_7NFSK9.

[12] LEYLAND, M.J., *et al.*, "Pedestal width study in dense high triangularity ELMy H-mode plasmas on JET," in preparation (2012).

[13] BURRELL, K.H., *et al.*, Plasma Phys. Control. Fusion **44** (2002) A253; Plasma Phys. Control. Fusion **47** (2005) B37.

[14] EVANS, T.E., *et al.*, Phys. Rev. Lett. **92** (2004) 235003; Nature Phys. **2** (2006) 419.

[15] FERRARO, N.M., Phys Plasmas **19** (2012) 056105, and references therein.

[16] FERRARO, N.M, *et al.*, "Edge plasma response to non-axisymmetric fields in tokamaks", this meeting TH/P4-21 (2012).

[17] WADE, M.R., *et al.*, "Advances in the physics understanding of ELM suppression using RMP on DIII-D," this meeting EX/3-1 (2012).

[18] WANG, E., *et al.*, "Linear gyrokinetic analysis of a DIII-D H-Mode pedestal near ideal ballooning threshold," to appear in Nucl. Fusion, 2012.

[19] DICKINSON, D., *et al.*, Plasma Phys. Control. Fusion **53** (2011) 115010.

[20] WAN, W., *et al.*, "Global gyrokinetic simulation of tokamak edge pedestal instabilities," submitted to Phys. Rev. Lett., 2012.

ACKNOWLEDGMENT